**AFRL-AFOSR-VA-TR-2024-0145**

Absolute Instability of Interacting Planar Mixing Layers and Wakes

**Alves, Leonardo**
**UNIVERSITY FEDERAL FLUMINENSE**
**RUA MIGUEL DE FRIAS 09**
**ICARAI NITEROI, , RJ 24220**
**BR**

**02/05/2024**
**Final Technical Report**

**DISTRIBUTION A: Distribution approved for public release.**

Air Force Research Laboratory
Air Force Office of Scientific Research
Arlington, Virginia 22203
Air Force Materiel Command

# REPORT DOCUMENTATION PAGE

**PLEASE DO NOT RETURN YOUR FORM TO THE ABOVE ORGANIZATION.**

| **1. REPORT DATE** | **2. REPORT TYPE** | **3. DATES COVERED** | |
|---|---|---|---|
| 20240205 | Final | **START DATE** 20201201 | **END DATE** 20221130 |

**4. TITLE AND SUBTITLE**
Absolute Instability of Interacting Planar Mixing Layers and Wakes

| **5a. CONTRACT NUMBER** | **5b. GRANT NUMBER** | **5c. PROGRAM ELEMENT NUMBER** |
|---|---|---|
| | FA9550-20-1-0359 | |
| **5d. PROJECT NUMBER** | **5e. TASK NUMBER** | **5f. WORK UNIT NUMBER** |
| | | |

**6. AUTHOR(S)**
Leonardo Alves

**7. PERFORMING ORGANIZATION NAME(S) AND ADDRESS(ES)**
UNIVERSITY FEDERAL FLUMINENSE
RUA MIGUEL DE FRIAS 09
ICARAI NITEROI RJ 24220
BR

**8. PERFORMING ORGANIZATION REPORT NUMBER**

| **9. SPONSORING/MONITORING AGENCY NAME(S) AND ADDRESS(ES)** | **10. SPONSOR/MONITOR'S ACRONYM(S)** | **11. SPONSOR/MONITOR'S REPORT NUMBER(S)** |
|---|---|---|
| Air Force Office of Scientific Research<br>875 N. Randolph St. Room 3112<br>Arlington, VA 22203 | AFRL/AFOSR IOS | AFRL-AFOSR-VA-TR-2024-0145 |

**12. DISTRIBUTION/AVAILABILITY STATEMENT**
A Distribution Unlimited: PB Public Release

**13. SUPPLEMENTARY NOTES**

**14. ABSTRACT**
Experiments, direct numerical simulations and stability analyses found in the literature for asymmetric wakes have consistently stated that only a single self-sustaining frequency exists and it is associated with an absolutely unstable wake, where the mixing-layer mode remains convectively unstable. This report presents evidence from experiments (FA9550-21-1-0052) as well as linear stability analyses (FA9550-20-1-0359) suggesting that the mixing- layer mode can become absolutely unstable as well, but only under certain parametric conditions involving appropriate velocity and length scales. These conditions 0<<VR<<1, theta_2>>theta)1 as well as theta_1<<1 and theta_2<<1. The first one constrains the velocity ratio between slow and fast streams to values much higher than pure mixing-layer (VR = 0) and much lower than symmetric wakes (VR = 1) conditions. The second one constrains the dimensionless momentum thickness of the slow stream to be much larger than its fast stream counterpart. Finally, the last two ones constrain both momentum thicknesses to be much smaller than the splitter plate thickness. Under these conditions, the flow becomes self-excited
with two distinct and independent frequencies. This discovery has important implications to mixing efficiency and combustion instabilities, affecting the design of injection systems that employ coaxial jets with a thick inner nozzle wall, which are commonly used by the United States Air Force.

**15. SUBJECT TERMS**

| **16. SECURITY CLASSIFICATION OF:** | | | **17. LIMITATION OF ABSTRACT** | **18. NUMBER OF PAGES** |
|---|---|---|---|---|
| **a. REPORT** | **b. ABSTRACT** | **c. THIS PAGE** | SAR | 25 |
| U | U | U | | |

| **19a. NAME OF RESPONSIBLE PERSON** | **19b. PHONE NUMBER** *(Include area code)* |
|---|---|
| ROGER GREENWOOD | 000-000-0000 |

**Standard Form 298** (Rev.5/2020)
Prescribed by ANSI Std. Z39.18

# REPORT DOCUMENTATION PAGE

*Form Approved*
*OMB No. 0704-0188*



| **1. REPORT DATE** *(DD-MM-YYYY)* | **2. REPORT TYPE** | **3. DATES COVERED** *(From - To)* |
|---|---|---|
| 15/01/2024 | Final Performance Report | 18/11/2021 - 28/02/2023 |

**4. TITLE AND SUBTITLE**

Absolute Instability of Interacting Planar Mixing Layers and Wakes

**5a. CONTRACT NUMBER**

**5b. GRANT NUMBER**

FA9550-20-1-0359

**5c. PROGRAM ELEMENT NUMBER**

**6. AUTHOR(S)**

Alves, Leonardo S. de B.

**5d. PROJECT NUMBER**

**5e. TASK NUMBER**

**5f. WORK UNIT NUMBER**

**7. PERFORMING ORGANIZATION NAME(S) AND ADDRESS(ES)**

Universidade Federal Fluminense,
Rua Miguel de Frias, 9,
Icaraí, Niterói, RJ 24220-900, Brazil

**8. PERFORMING ORGANIZATION REPORT NUMBER**

**9. SPONSORING/MONITORING AGENCY NAME(S) AND ADDRESS(ES)**

Roger Greenwood
Souther Office of Aerospace Research & Development,
Air Force Office of Scientific Research,
Las Condes, Santiago, Chile

**10. SPONSOR/MONITOR'S ACRONYM(S)**

SOARD/AFOSR

**11. SPONSOR/MONITOR'S REPORT NUMBER(S)**

**12. DISTRIBUTION/AVAILABILITY STATEMENT**

Approved for public release, distribution unlimited.

**13. SUPPLEMENTARY NOTES**

**14. ABSTRACT**

Experiments, direct numerical simulations and stability analyses found in the literature for asymmetric wakes have consistently stated that only a single self-sustaining frequency exists and it is associated with an absolutely unstable wake, where the mixing-layer mode remains convectively unstable. This report presents evidence from experiments (FA9550-21-1-0052) as well as linear stability analyses (FA9550-20-1-0359) suggesting that the mixing- layer mode can become absolutely unstable as well, but only under certain parametric conditions involving appropriate velocity and length scales. These conditions are $0 \ll VR \ll 1$, $\theta_2 \gg \theta_1$ as well as $\theta_2 \ll 1$ and $\theta_1 \ll 1$. The first one constrains the velocity ratio between slow and fast streams to values much higher than pure mixing-layer ($V R = 0$) and much lower than symmetric wakes ($V R = 1$) conditions. The second one constrains the dimensionless momentum thickness of the slow stream to be much larger than its fast stream counterpart. Finally, the last two ones constrain both momentum thicknesses to be much smaller than the splitter plate thickness. Under these conditions, the flow becomes self-excited with two distinct and independent frequencies. This discovery has important implications to mixing efficiency and combustion instabilities, affecting the design of injection systems that employ coaxial jets with a thick inner nozzle wall, which are commonly used by the USAF.

**15. SUBJECT TERMS**

| **16. SECURITY CLASSIFICATION OF:** | | | **17. LIMITATION OF ABSTRACT** | **18. NUMBER OF PAGES** | **19a. NAME OF RESPONSIBLE PERSON** |
|---|---|---|---|---|---|
| **a. REPORT** | **b. ABSTRACT** | **c. THIS PAGE** | | | |
| unclassified | unclassified | unclassified | UU | | **19b. TELEPHONE NUMBER** *(Include area code)* |

**Standard Form 298** (Rev. 8/98)

**Final Performance Report**
on

# Absolute Instability of Interacting Planar Mixing Layers and Wakes

*for*
*AFOSR Contract/Grant FA9550-20-1-0359*

**Prepared by**

**Leonardo S. de B. Alves**
**Principal Investigator**
**Departamento de Engenharia Mecânica,**
**Universidade Federal Fluminense,**
**Rua Passo da Pátria 156, Escola de Engeharia,**
**São Domingos, Niterói, RJ 24210-240, Brazil**

**Submitted to**

**Roger Greenwood**
**Director**
**Southern Office of Aerospace Research & Development**
**Air Force Office of Scientific Research**
**Av. Andres Belo, 2800,**
**Las Condes, Santiago, Chile**

February 28th, 2023

## Executive Summary

Experiments, direct numerical simulations and stability analyses found in the literature for asymmetric wakes have consistently stated that only a single self-sustaining frequency exists and it is associated with an absolutely unstable wake, where the mixing-layer mode remains convectively unstable. This report presents evidence from experiments (FA9550-21-1-0052) as well as linear stability analyses (FA9550-20-1-0359) suggesting that the mixing-layer mode can become absolutely unstable as well, but only under certain parametric conditions involving appropriate velocity and length scales. These conditions are $0 \ll VR \ll 1$, $\theta_2 \gg \theta_1$ as well as $\theta_2 \ll 1$ and $\theta_1 \ll 1$. The first one constrains the velocity ratio between slow and fast streams to values much higher than pure mixing-layer ($VR = 0$) and much lower than symmetric wakes ($VR = 1$) conditions. The second one constrains the dimensionless momentum thickness of the slow stream to be much larger than its fast stream counterpart. Finally, the last two ones constrain both momentum thicknesses to be much smaller than the splitter plate thickness. Under these conditions, the flow becomes self-excited with two distinct and independent frequencies. This discovery has important implications to mixing efficiency and combustion instabilities, affecting the design of injection systems that employ coaxial jets with a thick inner nozzle wall, which are commonly used by the United States Air Force.

## Papers

D. B. Souza, H. Tanner, H. R. Quintanilha Jr, B. McKeon and L. S. de B. Alves, *Parametric conditions for dual-frequency self-excitation in asymmetric wakes*, **Journal of Fluid Mechanics**, In Preparation, 2024.

## Students Funded

Davi Bernhard de Souza, Post-Doc Position.
Helio Ricardo Quintanilha Junior, Post-Doc Position.

# Contents

# Chapter 1

# Introduction

## 1.1 Motivation

Coaxial jets are important in many engineering applications that require significant mixing between two fluid streams. For instance, their use is widespread in high-speed gas assisted spray formation, despite the complex mixing process involved (Villermaux and Rehab, 2000). They are also an integral part of the fuel and oxidizer injectors in many propulsion systems, such as liquid rocket engines (Oschwald et al., 2006), and have even been recently studied in the context of air-breathing engines (Harris et al., 2020). This work focussed on the particular case where the inner nozzle wall is thick, since this is the case of the coaxial injectors used by the Cryogenic Supercritical Laboratory at AFRL Edwards (Leyva et al., 2007).

## 1.2 Literature Review

### 1.2.1 Coaxial Jets

One seldom investigated feature of the aforementioned geometry is the thickness of the inner nozzle wall at the coaxial jet exit. It has an important effect on the resulting coaxial jet linear and modal instability. On one hand, this wall is usually assumed sufficiently thin. In this case, the mixing-layer mode associated with an incompressible and isothermal coaxial jet is convectively unstable (Michalke and Hermann, 1982). Applying enough suction through the outer nozzle, however, transitions this mixing-layer mode towards absolute instability (Strykowski and Niccum, 1991), promoting significant mixing enhancement (Strykowski and Wilcoxon, 1993). On the other hand, the inner nozzle wall is thick in many relevant geometries. Experimental studies of similar geometries have suggested the presence of vortex shedding from the inner wall (Buresti et al., 1994), which indicates the existence of an annular and asymmetric wake. Theoretical studies of similar geometries have confirmed these findings by identifying an absolute instability of a wake mode in the coaxial jet near field (Michalke, 1993; Talamelli and Gavarini, 2006).

### 1.2.2 Asymmetric Wakes

The canonical model for such flows is the planar mixing-layer that forms downstream of a thick splitter plate. Experimental studies by Boldman et al. (1976) have long shown the presence of vortex shedding at a frequency that scales with plate thickness and mean velocity when the velocity ratio between fast and slow streams approaches one (symmetric wake), but becomes weaker and eventually disappears as this ratio approaches zero (pure mixing-layer). Theoretical studies of these planar and asymmetric wakes by Koch (1985) and Wallace and Redekopp (1992) explain this behavior through the influence of the velocity ratio as well as boundary-layer and plate thicknesses on the convective/absolute nature (Huerre and Monkewitz, 1990) of the wake mode instability, while the mixing-layer mode remains convectively unstable. This understanding was then confirmed using direct numerical simulations by Hammond and Redekopp (1997) and Laizet et al. (2010).

Recently, experiments performed by Tian et al. (2012) provided some evidence for the existence of two self-excited frequencies under a limited number of parametric conditions for this canonical problem. The theoretical study by Quintanilha Jr and Alves (2018) then showed that this was likely due to the mixing-layer mode becoming absolutely unstable as well for these conditions. Both studies, however, are far from being conclusive. On one hand, the former was not designed to generate accurate spectra. Hence, the existence of this second frequency is questionable. On the other hand, the latter reconstructed the base flow used in their stability analysis with an image processing technique employed to extract the mean stream wise velocity profile from the PIV images of the former. Hence, their accuracy is also questionable.

## 1.3 Objectives

This report discusses how the aforementioned shortcomings were overcome to confirm the existence of a dual-frequency excitation. All experimental work discussed here was performed by the CalTech group led by prof. Beverley McKeon, funded by AFOSR under grant FA9550-21-1-0052. They performed experiments that were specifically designed to provide accurate mean flows as well as accurate spectra for the parametric conditions where both wake and mixing-layer modes were most likely absolutely unstable according to their corresponding stability analyses. The latter theoretical work was performed by the UFF group led by prof. LeoAlves.

# Chapter 2

# Methodology

The model employed in this study uses the unsteady, two-dimensional and constant property incompressible Navier-Stokes equations. They are written in dimensionless form using the splitter plate thickness and upper stream velocity as length and velocity scales, which are also employed to build time and pressure scales. This leads to the Reynolds number $Re$, the lower to upper layer velocity ratio $VR$ as well as the upper and lower layers momentum thicknesses $\theta_1$ and $\theta_2$, respectively, as dimensionless parameters. A linear, local and modal stability analysis is then performed to improve our understanding of the coherent structures found in the experimental results. In order to do so, however, appropriate base flows have to be defined first. This is discussed next.

## 2.1 Base Flow Analysis

Two base flows were employed for this study. They were constructed by applying two different fitting procedures to the mean velocity data measured in the experiments. These base flows, however, contain only the mean stream wise velocity component. The mean transversal velocity component was neglected. This is due to the fact that a local and, hence, parallel approximation is employed in the present linear and modal stability analysis. Both fitting procedures are described next.

### 2.1.1 Fourier Filter

A third-order polynomial interpolation of the mean data is the first base flow used. It was obtained with the namesake built-in function of the software *Mathematica* (Wolfram, 2003). Doing so, however, presents a couple of challenges.

First, applying interpolation algorithms directly to the raw experimental data to construct base flows led to the appearance of spurious modes in our stability calculations. This was due to the resulting functions being plagued by high wave number oscillations. Fourier filtering was then used to greatly minimize this issue (Brigham, 1974). The idea is to Fourier transform the raw data and then truncate the summation process of the inverse transform in order to keep out the high wave number eigenvectors where the aforementioned oscillations take place.

The second challenge is that mean flows are not solutions of the steady governing equations. Hence, they can introduce not only quantitative but also qualitative errors in stability analyses (Teixeira and Alves, 2017). Nevertheless, they have been successfully used as base flows in linear stability analyses to predict the frequency content of symmetric wakes (Pier, 2002; Barkley, 2006; Thiria and Wesfreid, 2007) likely because the mean wake weakly nonlinear behavior is marginally stable (Sipp and Lebedev, 2007).

### 2.1.2 Boundary-Layer Filter

Motivated by the aforementioned issues associated with the use of a mean flow as base flow in a stability analysis, a second base flow was developed. The procedure employed to do so is based on similarity solutions of the boundary-layer equations. They are obtained with the shooting method, implemented using the built-in functions **NDSolve** and **FindRoot** from the software *Mathematica* (Wolfram, 2003) for the initial value problem and search procedure, respectively. Their parameters, however, are still adjusted using a separate search procedure for them to fit the mean flow data.

The first step of this procedure obtains similarity solutions of the classical Blasius equation (Schlichting, 1986). Doing so requires providing the dimensional parametric conditions associated with the mixing-layers that develop downstream of both sides of the splitter plate, namely the dynamic viscosity, both free-stream (mean) velocities as well as the minimum (mean) velocity near the centerline. An optimization step is then required to identify the best stream wise position in the similarity solution, where the objective function measures the difference between this solution and the experimental data at the stream wise position of interest. This effectively finds the optimal momentum thicknesses of the mixing-layers downstream of each side of the splitter plate. The second step of this procedure combines both solutions into a single uniformly valid solution, as accurate as any boundary-layer solution, using the method of matched asymptotic expansions (Dyke, 1964; Cole, 1968). A similar procedure has already been successfully applied to generate approximate base flows for the jet in crossflow (Kelly and Alves, 2008).

Although this second base flow does not match the experimental data as well as the first one, it does have two important advantages. One is the fact that this base flow is not a mean flow, but an accurate solution of the boundary-layer equations that fits the mean flow data. Hence, it more closely resembles a steady-state than a mean flow. Two is the fact that this base flow has adjustable parameters. Hence, it is possible to accurately estimate what the base flow would look like at parametric conditions that slightly differ from the experimental ones. This, in turn, can be used to improve our understanding of the physical mechanisms that drive the experimentally observed phenomenon.

## 2.2 Stability Analysis

Having defined base flows that adequately represent the experiment currently under investigation, a stability analysis can be employed to describe the unstable coherent structures that emerge from these base flows, under the constraint of the chosen model for the flow governing equations. This analysis is linear, i.e. it assumes that these structures arise from small amplitude disturbances. This analysis is also local, i.e. it assumes the disturbance eigenfunctions do not depend on the stream wise coordinate. Enforcing such a constraint requires neglecting the base flow derivatives with respect to the stream wise coordinate, which is equivalent to imposing the well-known parallel flow hypothesis since this is a two-dimensional incompressible flow model. Finally, this analysis is modal as well, i.e. it assumes the time-asymptotic exponential behavior of these disturbances is the dominant one controlling their growth or decay. These assumptions result in the disturbances having a wave-like behavior in both time and stream wise coordinates, leaving the transversal direction as the only inhomogeneous one. Hence, their governing equation is given by the well-known Orr-Sommerfeld equation (Schmid and Henningson, 2001). Two methods are used to solve it. They have been recently employed in the context of free and transverse jets (Souza et al., 2021) and are discussed in detail next.

### 2.2.1 Shooting Method

The first one is an advanced version of the standard shooting method. On one hand, the standard version was implemented using the software *Mathematica* (Wolfram, 2003) built-in functions **NDSolve** and **FindRoot** for the initial value problem and search procedure, respectively. It was fist employed to solve the Rayleigh equation for an incompressible jet in crossflow (Alves et al., 2008). Improvements have been implemented since then, allowing its use in many other complex stability problems. An example is the mixed convection of viscoelastic fluids (Hirata et al., 2015). On the other hand, the advanced version solves both direct and adjoint problems together in order to facilitate the search for saddle-points and, hence, the identification of absolute instabilities (Alves et al., 2019). This variation has been successfully applied for this purpose in the context of separated boundary-layers (Avanci et al., 2019) and flows in porous media (Schuabb et al., 2020).

### 2.2.2 Matrix Forming

Identifying the onset of absolute instability, however, requires an additional step. One must make sure that the saddle-point found using the previous method is, in fact, a pinching-point as well. In order to do so, the collision criterion originally derived by Briggs (1964) is employed. The second method, generally known as matrix forming, was employed here to verify this criterion. Before doing so, a few preliminary steps are required. First, the nonlinear differential eigenvalue problem for the stream wise wave number is re-written as a linear differential eigenvalue problem using the companion matrix method (Bridges and Morris, 1984). Sixth-order central difference schemes are then applied to all spatial derivatives in this equation, transforming it into an algebraic generalized eigenvalue problem. Finally, the shift-and-invert Arnoldi method (Saad, 2003) is employed to generate the Hessenberg matrix, whose Ritz values are calculated in Fortran with the **ZGEEV** subroutine from **LAPACK** (Anderson et al., 1999).

One more thing must be mentioned before ending this subsection. The matrix forming method is also employed in the present work to generate initial guesses for the shooting method, facilitating the search for any physically meaningful modes that might exist.

# Chapter 3

# Base Flow Results

Mean stream wise and transversal velocity components were obtained from experiments performed by the CalTech research group, led by prof. McKeon and funded under a separate grant by AFOSR (FA9550-21-1-0052). Two different filtering procedures were then employed to this data as part of the present work to generate sufficiently smooth velocity profiles. They were then employed as base flows in the the stability analyses discussed in the next chapter. These procedures were discussed in the previous chapter. In the following sections, a few results are shown to illustrate their quality.

## 3.1 Fourier Filter

This section focusses on the base flows that were obtained when applying the filtering procedure based on Fourier transforms to the experimental data. Since this procedure is well known and was already discussed in detail on section 2.1.1, only a few results are shown here for the sake of completeness. Figure 3.1 show the mean stream wise velocity profiles obtained for $VR \simeq 0.5$ and $Re \simeq 15,000$, including (left) experimental and filtered wall normal profiles at $x/t = 2.0916$ and (right) the full filtered profile as a function of the stream wise and wall normal coordinates. On one hand, the former shows that the filtering effect of removing all high wave number data produces no

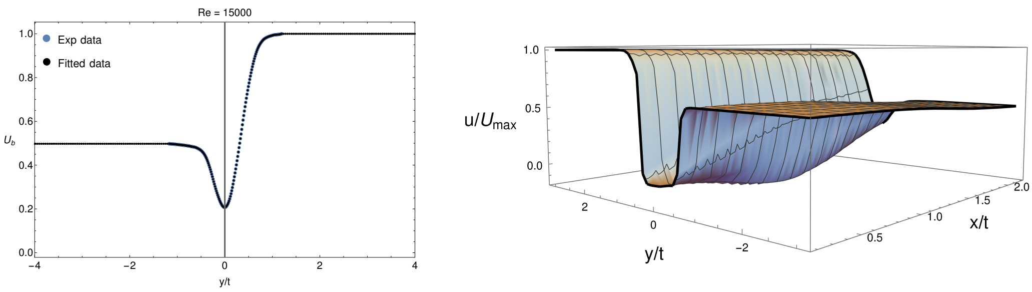


Figure 3.1: Mean stream wise velocity profiles for $VR \simeq 0.5$ and $Re \simeq 15,000$, including (left) the wall normal profile at $x/t = 2.0916$ and (right) the fully filtered two-dimensional profile.

visible changes to the original data, compared to the original experimental data. On the other hand, the latter plot suggests that the flow is indeed slowly diverging near the splitter plate. This changes further downstream because the potential core region ends approximately just before one splitter plate thickness. Beyond this point, stream wise gradients are clearly more significant due to the increased mixing between both streams. It is possible to anticipate numerical issues when using this profile, however, due to the stream wise oscillations that can be observed in the latter plot.

## 3.2 Boundary-Layer Filter

This chapter ends by repeating the previous analysis but now focussing on the boundary-layer filtering procedure. As already mentioned in section 2.1.2, the main difference between both filters is the fact that the previous one still generates a mean solution, albeit smoothed out, while the present one can be considered a steady-state as accurate as any solution of the boundary-layer equations. Sample results obtained for the boundary-layer filter are shown in Fig. 3.2, which is analogous to Fig. 3.1. As one would expect, this figure (left) shows that it doesn't match the experimental data as accurately, which is the price paid for representing a steady profile. On the other hand, this figure (right) also shows that its profile is smoother both in the wall normal and stream wise directions. Such a difference between both profiles manifests itself on the stability results as well, which are discussed next.

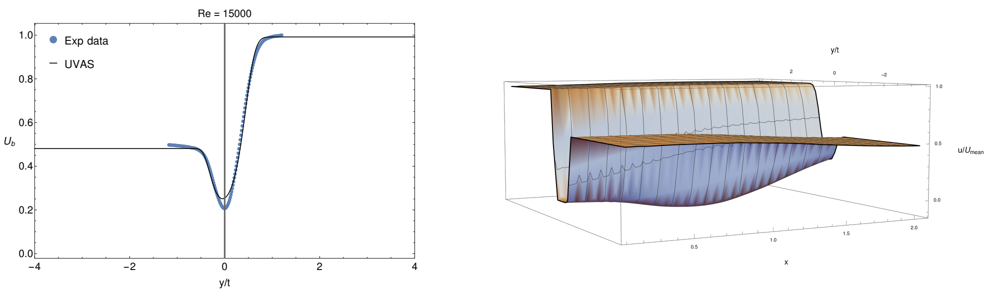


Figure 3.2: Same as Fig. 3.1, but for the boundary-layer filter.

# Chapter 4

# Stability Results

Previous studies guided the selection of the parametric conditions used to design the first experimental campaign (Tian et al., 2012; Quintanilha Jr and Alves, 2018). Its mean flow data was extracted for the theoretical studies employed to explain its spectra. This theoretical analysis was then employed to design the second experimental campaign, which confirmed the trends observed. These steps are described in detail next.

## 4.1 First Campaign

### 4.1.1 Experimental Data

Data sets generated by the CalTech group under grant FA9550-21-1-0052 for $VR \simeq 0.5$ were first post-processed by them to verify the existence of two self-excited frequencies. This was done by plotting the power spectral density extracted from the wall normal velocity disturbance component downstream of the splitter plate, as shown in Figure 4.1 when measured at (left) $y = 0.076$ for $Re \simeq 15,000$ and at (right) $y = 0.146$ for $Re \simeq 24,000$. Two distinct and independent frequencies can be observed in both cases. The frequency with a higher (lower) amplitude has a Strouhal number of $St \simeq 0.29$ (0.26) and 0.27

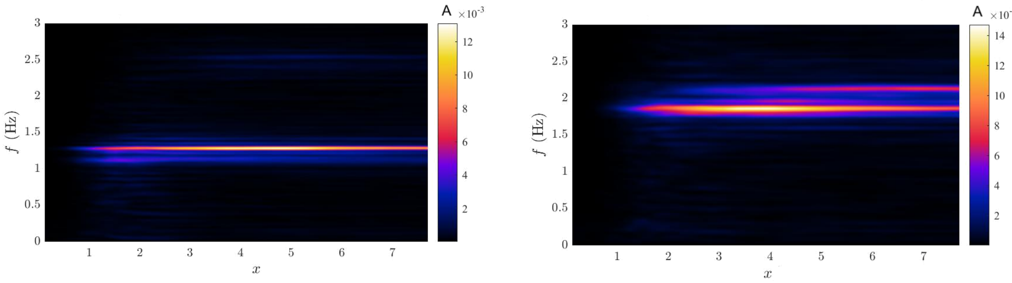


Figure 4.1: Power spectral density obtained from the wall normal velocity disturbance measured during the first experimental campaign with $VR \simeq 0.5$ (left) for $Re \simeq 15,000$ at $y = 0.076$ and (right) for $Re \simeq 24,000$ at $y = 0.146$. Splitter plate ends at $x = 0$.

(0.31) on the left and right plots, respectively. It is well-known that the wake mode is weakly dependent on large Reynolds numbers whereas the mixing-layer mode is strongly dependent on the momentum thickness, which becomes smaller as the Reynolds number increases due to its relation to the splitter plate boundary-layer thickness. Hence, the Strouhal number with a low (high) amplitude likely belongs to the mixing-layer (wake) mode. Detailed theoretical support for this hypothesis is provided in the next subsection.

### 4.1.2 Theoretical Analysis

Having confirmed the presence of two distinct and independent frequencies in the first campaign experimental data, a theoretical analysis of this data set can be pursued. This is done by following the procedures described in section 2.2. Doing so leads to the results shown in Figure 4.2 for the locally absolute temporal growth rate as a function of the stream wise location, i.e. $Im[\omega_0(x)]$, when $VR \simeq 0.5$ as well as (left) $Re \simeq 15,000$ and (right) $Re \simeq 24,000$. Solid and dashed lines respectively represent results from the first and second campaigns, although the latter is only discussed in the next section. The black and orange curves represent the wake and mixing-layer modes, respectively. This nomenclature is still guided by the assumption that the former is the dominant one and, hence, must have the highest growth rate. Vertical dashed lines mark the stream wise region of absolute instability, i.e. $\Delta x_A = x_2 - x_1 > 0$ where $Im[\omega_0(x_1)] = Im[\omega_0(x_2)] = 0$ and $Im[\omega_0(x_1 < x < x_2)] > 0$. Finally, the big dots in black and orange respectively represent the wake and mixing-layer weakly global growth rates, defined here as the highest locally absolute temporal growth rate of each mode (Huerre and Monkewitz, 1990). The word weakly is used here to distin-

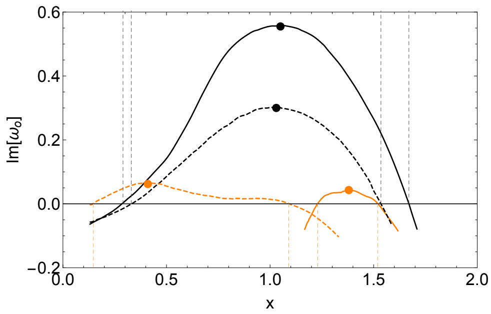


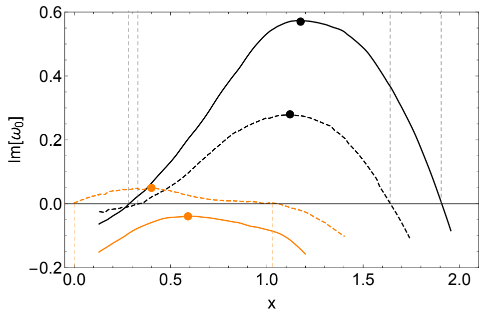


Figure 4.2: Locally absolute temporal growth rate calculated using the Fourier filtered base flow at each stream wise location downstream of the splitter plate when $VR \simeq 0.5$ as well as (left) $Re \simeq 15,000$ and (right) $Re \simeq 24,000$. The large dots in black and orange represent the wake and mixing-layer global growth rates, respectively. Solid and dashed curves respectively represent results from the first and second campaigns. Finally, light vertical dashed lines mark the stream wise region of absolute instability of each mode.

guish the present essentially local analysis from truly global ones (Theofilis, 2011). A few important conclusions can be drawn about the first campaign. First, even though the noise levels in the stability data when using Fourier filtered base flow was much lower than in previous studies (Quintanilha Jr and Alves, 2018), attesting to the quality of the experimental data and theoretical procedures employed here, they were still too high. Hence, this base flow was not used here. Second, as expected, the region of absolute instability of the wake mode starts just downstream of the splitter plate, whereas the mixing-layer one is significantly smaller and starts much further downstream. The third and final result is the weakening of the mixing-layer mode absolute instability when the Reynolds number is increased, to the point of making it marginally absolutely stable, which goes against experimental trends. Although not shown here, similar trends are observed with the Fourier filtered base flow. This could be due to the local assumption, given the strong nonlocal behavior of the base flow near the splitter plate where the least weakly globally stable mode is located.

Up to this point, the high (low) amplitude frequency in the experimental data as well as the high (low) weakly global growth rate in the theoretical analysis have been related to the wake (mixing-layer) mode based on the known behavior of the symmetric wake (pure mixing-layer) mode. A more rigorous justification for this nomenclature can be provided by comparing their respective eigenfunctions. This is done in Figure 4.3 for the high (left) and low (right) amplitude modes. The comparison is performed for the parametric conditions specified for the large black and orange dots in Figure 4.2 (left). Both plots in Figure 4.3 show a clear similarity between respective pressure eigenfunctions, providing additional evidence that the second self-excited frequency observed in the experiments is indeed due to the absolute instability of the mixing-layer mode when $Re \simeq 15,000$.

It is then important to try and understand why the absolute instability of the mixing-layer mode was not theoretically observed when $Re \simeq 24,000$. In order to do so, a detailed analysis of the boundary-layer filtered base flow

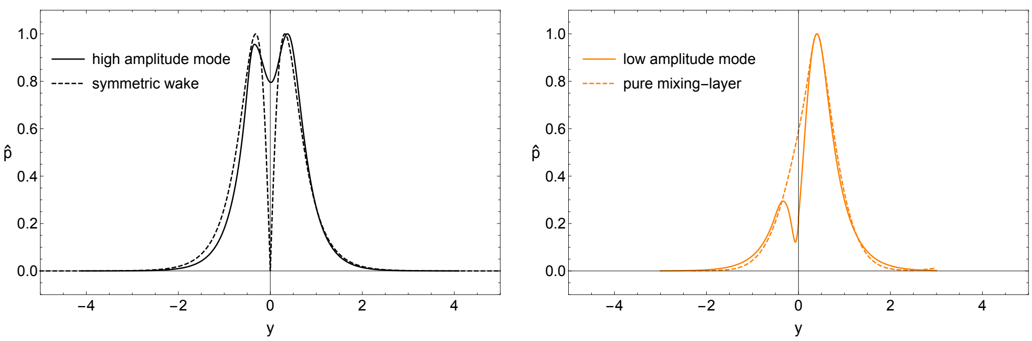


Figure 4.3: Pressure eigenfunction comparison between (left) high amplitude mode and symmetric wake as well as (right) low amplitude mode and pure mixing-layer for the weakly global parametric conditions of the Fourier filtered base flow with $Re \simeq 15,000$.

parameters was performed. Since this instability will not occur in the known velocity ratio limits, namely for the pure mixing-layer ($VR = 0$) and the symmetric wake ($VR = 1$), it is reasonable to expect that it will be observed when $0 \ll VR \ll 1$. Hence, the present analysis focuses on the influence of the dimensionless momentum thicknesses $\theta_1$ and $\theta_2$ when $VR = 0.5$. This is done in Figure 4.4, which shows the locally absolute temporal growth rate of both modes as a function of one of the momentum thicknesses while the other is kept constant. It also shows blue circles to indicate the parametric region of the first experimental campaign. This result suggests an explanation as to why the mixing-layer mode is marginally absolutely unstable (stable) when $Re \simeq 15,000$ ($Re \simeq 24,000$). Furthermore, this figure suggests that the absolute instability of the mixing-layer mode can be made stronger by increasing the momentum thickness of the slower layer, without significantly weakening the absolute instability of the wake mode. In order to test this hypothesis, a second campaign was undertaken.

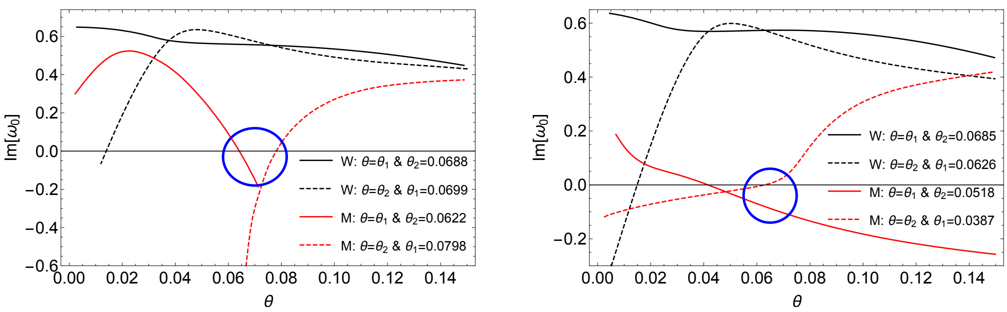


Figure 4.4: Locally absolute temporal growth rate of the wake (W) and mixing-layer (M) modes, calculated using the boundary-layer filtered base flow, as a function of one of the momentum thicknesses while the other is kept constant at the weakly global point for $VR \simeq 0.5$ as well as (left) $Re \simeq 15,000$ and (right) $Re \simeq 24,000$. Solid (dashed) lines are for a constant $\theta_2$ ($\theta_1$). The blue circles mark the first campaign parametric regions.

## 4.2 Second Campaign

### 4.2.1 Experimental Data

The procedures described under grant FA9550-21-1-0052 and the first campaign measurements presented in subsection 4.1.1 were repeated in the second campaign, with only one modification. In order to increase the momentum thickness $\theta_2$, the lower stream boundary-layer forming under the splitter plate was tripped to increase its thickness. The power spectral density was extracted from the wall normal velocity disturbance and shown in Figure 4.5. Once again, two distinct and independent frequencies are observed, with the originally high (low) amplitude one having a lower (higher) amplitude for both Reynolds numbers.

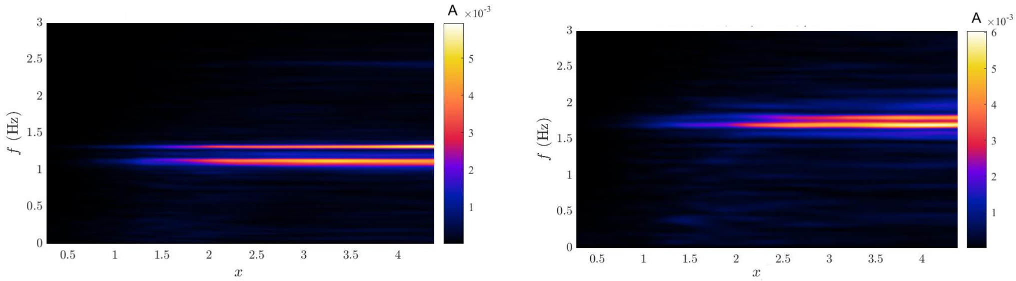


Figure 4.5: Same as Figure 4.1, but for the second campaign data.

### 4.2.2 Theoretical Analysis

Some of these second campaign trends are consistent with the dashed curves already suggested by Figure 4.4. This is true even though these curves do not represent the dependence of weakly global modes on the momentum thicknesses, but the dependence of the locally absolute modes instead. For instance, not only the wake mode has a smaller amplitude for both Reynolds numbers but also the mixing-layer mode is weakly globally unstable for both Reynolds numbers.

# Chapter 5

# Epilogue

## 5.1 Conclusions

Combined results from experiments, direct numerical simulations as well as linear stability analyses have all long suggested that asymmetric wakes have a single self-sustained frequency associated with an absolute instability of the wake mode, whereas the mixing-layer mode remains convectively unstable. The present report provided evidence from linear stability analyses to explain the experimental data provided under grant FA9550-21-1-0052 suggesting that the mixing-layer mode can also become absolutely unstable under appropriate parametric conditions. This was only possible in the present analysis when three conditions were met. First, the velocity ratio is between the pure mixing-layer and symmetric wake limits, namely $0 \ll VR \ll 1$. Second, the momentum thickness associated with the boundary-layer thickness of the slow stream must be much larger than its faster counterpart, namely $\theta_2 \gg \theta_1$. Third, it is important to note that both momentum thicknesses were much smaller than the splitter plate thickness in the present study, namely $\theta_2 \ll 1$ and $\theta_1 \ll 1$. The possibility of dual-frequency self-excitation in the interaction between mixing-layers and wakes could have importante consequences towards the original problem that motivated this study, namely the design of the coaxial jets used by injectors in propulsion systems of interest to the US Air Force, in order to avoid undesired mixing and combustion instabilities.

## 5.2 Future Work

Despite the importance of this finding, namely that the mixing-layer mode in asymmetric wakes can also become absolutely unstable, the present analysis can still be improved upon in a few different ways. This is necessary not only to make it more accurate but also to extend it to coaxial jets. These improvements are discussed next.

### 5.2.1 Short Term Improvements

One important analysis was kept out of the previous chapters of this report, namely a comparison between the experimental and theoretical spectra. This is presented now in Figure 5.1 using the Fourier filtered base flow for $VR \simeq 0.5$ as well as (left) $Re \simeq 15,000$ and (right) $Re \simeq 24,000$, using the dimensionless angular frequency instead. Each colored curve represents an experimental spectrum measured at a different stream wise location downstream of the splitter plate. Theoretical results are included in two separate ways. Black (orange) dashed vertical lines indicate the weakly global angular frequencies of the wake (mixing-layer) mode, whereas light black (orange) bars indicate the frequency range of the locally absolutely unstable region. Before moving any further, it must be noted that there should not be an orange dashed vertical line and a light orange bar when $Re \simeq 24,000$, since theoretical results suggest the mixing-layer mode is absolutely stable as suggested by Fig. 4.2. Since this stability is only marginal and the data is noisy, however, the most likely line and bar for this case are included nonetheless. Nevertheless, the reason why this comparison was not presented before is clear. The quantitative agreement between theory and experiments is poor, although the deviations are not significant given the simplified nature of this analysis. In order to improve this comparison, two steps should be taken.

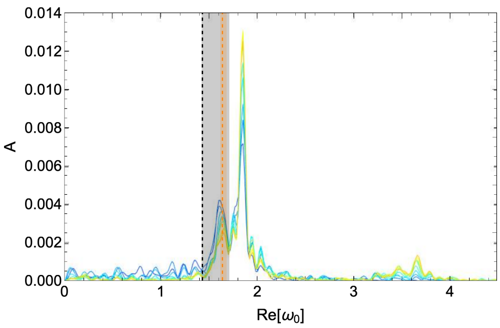


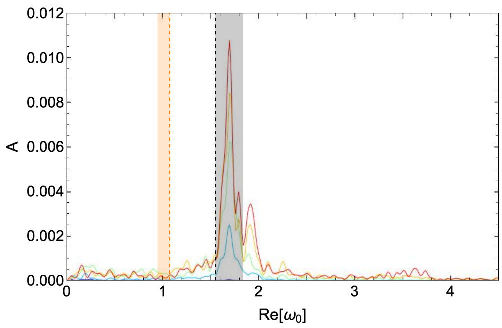


Figure 5.1: Spectra taken from Figure 4.1 at different locations downstream of the splitter plate. Theoretical results included as black (orange) dashed vertical lines that indicate the weakly global angular frequencies of the wake (mixing-layer) mode as well as light black (orange) bars that indicate the frequency range of the locally absolutely unstable region. The high Reynolds number mixing-layer results represent only a likely scenario.

#### Steady Base Flows

The first one will be the use of steady-states at transitional Reynolds numbers instead of mean turbulent flows as base flows for the stability analyses. Doing so prevents the linear analysis from being contaminated by nonlinear interactions between steady- states and disturbances that is present in mean flows. Accurate and disturbance free steady-states can be generated using an UFF *in-house* direct numerical simulation code. It was originally developed by Santos (2020) and recently improved upon by Silva (2023), during their respective PhD and MSc at UFF. This code was entirely built around the PETSc infrastructure and, hence, is highly scalable, presenting an essentially linear speed-up when using up to five thousand CPU cores. The thick splitter plate can be introduced using the cut-stencil method (Greene et al., 2016). An example of the current capabilities are shown in Fig. 5.2 for the unsteady supersonic two-dimensional flow around a circular cylinder, using reflective boundary conditions. This mesh is Cartesion and uniform, but the cylinder was superposed into it afterwards.

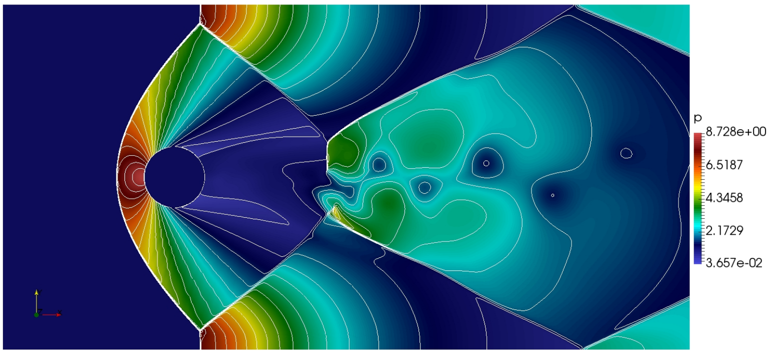


Figure 5.2: Pressure isocontours from the in-house direct numerical simulation code with cut-stencil used to solve the unsteady supersonic flow around a cylinder with reflective boundary conditions.

### Global Stability Analysis

The second one will be the use of a global instead of local stability analysis. Doing so should eliminate the errors introduced by neglecting the strong non-local and non-parallel behavior of base flow just downstream of the thick splitter plate. Both local and biGlobal linear and modal stability analyses

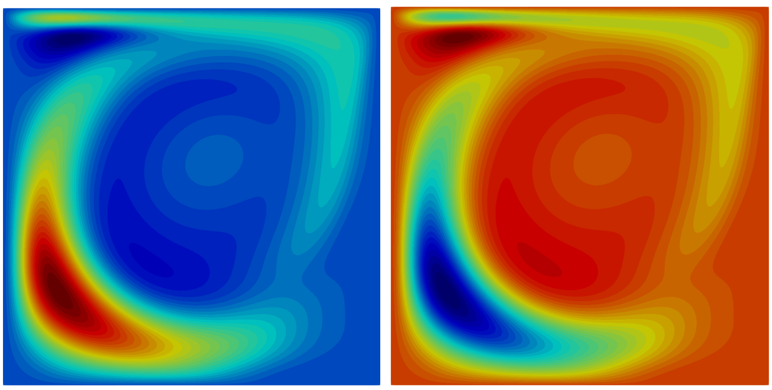

Figure 5.3: Real and imaginary stream wise velocity eigenfunction isocontours from the linear stability analysis code used to analyze the linear and global modes of the incompressible lid driven cavity problem.

can be performed using another UFF *in-house* code. It was originally developed and is still being improved upon by **?**, a former PhD student at UFF. This code is built around the PETSc/SLEPc infrastructure and its iterative nature significantly reduces memory constraints, a common issue in traditional matrix forming codes. An example of the current capabilities are shown in Fig. 5.3 for the real and imaginary stream wise velocity eigenfunction isocontours from the linear stability analysis code used to analyze the linear and global modes of the incompressible lid driven cavity problem.

### 5.2.2 Long Term Improvements

Both aforementioned capabilities are currently being implemented and should be ready to use quite soon. However, two major improvements must be added to the present capabilities in order to make this analysis applicable to the injection systems of interest to the US Air Force.

**Axial Symmetry:** The UFF in-house direct numerical simulation code can simulate planar two-dimensional and three-dimensional flows. However, an efficient generation of coaxial jet steady-states requires axially symmetric two-dimensional simulations. These are currently being implemented into this code.

**Compressibility Effects:** The UFF in-house linear and global stability code can simulate incompressible flows. However, in order to study these injection systems, the compressible flow equations must be used. This is currently being implemented into this code.

**Supercritical Fluids:** When designing injectors for liquid rocket engines, one must be able to mode the behavior of fluids whose thermodynamic state is near its critical point. Both in-house codes just mentioned can only simulate perfect gases. Hence, real gas models must be implemented as well, which is in our plans.

# References

L. S. de B. Alves, R. E. Kelly, and A. R. Karagozian. Transverse jet shear layer instabilities. part ii: Linear analysis for large jet-to-crossflow velocity ratios. *Journal of Fluid Mechanics*, 602:383–401, 2008. (Cited on page 5)

L. S. de B. Alves, S. C. Hirata, M. Schuabb, and A. Barletta. Identifying linear absolute instabilities from differential eigenvalue problems using sensitivity analysis. *Journal of Fluid Mechanics*, 870:941–969, 2019. (Cited on page 5)

E. Anderson, Z. Bai, C. Bischof, S. Blackford, J. Demmel, J. Dongarra, J. Du Croz, A. Greenbaum, S. Hammerling, A. McKenney, and D. Sorensen. *Lapack User's Guide*, volume 3rd. SIAM, 1999. (Cited on page 6)

M. P. Avanci, D. Rodríguez, and L. S. de B. Alves. A geometrical criterion for absolute instability in separated boundary layers. *Physics of Fluids*, 31 (014103), 2019. (Cited on page 5)

D. Barkley. Linear analysis of the cylinder wake mean flow. *Europhysics Letters*, 75(5):750–756, 2006. (Cited on page 4)

D. R. Boldman, P. F. Brinich, and M. E. Goldstein. Vortex shedding from a blunt trailing edge with equal and unequal external mean velocities. *Journal of Fluid Mechanics*, 75(4):721–735, 1976. (Cited on page 2)

T. J. Bridges and P. J. Morris. Differential eigenvalue problems in which the parameter appears nonlinearly. *Journal of Computational Physics*, 55: 437–460, 1984. (Cited on page 6)

R. J. Briggs. Electron-stream interaction with plasmas. Research Monograph 29, MIT, 1964. (Cited on page 5)

E. Brigham. *The Fast Fourier Transform.* Prentice-Hall Inc, Englewood Cliffs, NJ, 1974. (Cited on page 3)

G. Buresti, A. Talamelli, and P. Petagna. Experimental characterization of the velocity field of a coaxial jet configuration. *Experimental Thermal and Fluid Science*, 9:135–146, 1994. (Cited on page 1)

J. D. Cole. *Perturbation Methods in Applied Mathematics.* Blaisdell Publishing Company, Waltham, Massachusetts, 1968. (Cited on page 4)

M. V. Dyke. *Perturbation Methods in Fluid Mechanics*. Academic Press Inc., New York, United States, 1964. (Cited on page 4)

P. T. Greene, J. D. Eldredge, X. Zhong, and J. Kim. A high-order multi-zone cut-stencil method for numerical simulations of high-speed flows over complex geometries. *Journal of Computation Physics*, 316:652–681, 2016. (Cited on page 16)

D. A. Hammond and L. G. Redekopp. Global dynamics of symmetric and asymmetric wakes. *Journal of Fluid Mechanics*, 331:231–260, 1997. (Cited on page 2)

E. Harris, D. D. W. Ren, and A. R. Karagozian. Dynamics of coaxial transverse jets. In *APS Division of Fluid Dynamics*, 2020. (Cited on page 1)

S.da C. Hirata, L. S.de B. Alves, N. Delenda, and M. N. Ouarzazi. Convective and absolute instabilities in Rayleigh-Bénard-Poiseuille mixed convection for viscoelastic fluids. *Journal of Fluid Mechanics*, 765:167–210, 2015. (Cited on page 5)

P. Huerre and P. A. Monkewitz. Local and global instabilities in spatially developing flows. *Annual Review of Fluid Mechanics*, 22:473–537, 1990. (Cited on pages 2 and 10)

R. E. Kelly and L. S. de B. Alves. A uniformly valid asymptotic solution for the transverse jet and its linear stability analysis. *Philosophical Transactions of the Royal Society of London. Series A: Mathematical and Physical Sciences*, 366:2729–2744, 2008. (Cited on page 4)

W. Koch. Local instability characteristics and frequency determination of self-excited wake flows. *Journal of Sound and Vibration*, 99(1):53–83, 1985. (Cited on page 2)

S. Laizet, S. Lardeau, and E. Lamballais. Direct numerical simulation of a mixing layer downstream a thick splitter plate. *Physics of Fluids*, 22 (015104), 2010. (Cited on page 2)

I. A. Leyva, B. Chehroudi, and D. Talley. Dark core analysis of coaxial injectors at sub-, near-, and supercritical pressures in a transverse acoustic field. In *43rd AIAA/ASME/SAE/ASEE Joint Propulsion Conference & Exhibit*, number AIAA 2007-5456, 2007. (Cited on page 1)

A. Michalke. On the influence of a wake on the inviscid instability of a circular jet with external flow. *European Journal of Mechanics: B Fluids*, 12(5):579–595., 1993. (Cited on page 1)

A. Michalke and G. Hermann. On the inviscid instability of a circular jet with external flow. *Journal of Fluid Mechanics*, 114:343–359, 1982. (Cited on page 1)

M. Oschwald, J. J. Smith, R. Branam, J. Hussong, A. Schik, B. Chehroudi, and D. Talley. Injection of fluids into supercritical environments. *Combustion Science and Technology*, 178(1):49–100, 2006. (Cited on page 1)

B. Pier. On the frequency selection of finite-amplitude vortex shedding in the cylinder wake. *Journal of Fluid Mechanics*, 458:407–, 2002. (Cited on page 4)

H. R. Quintanilha Jr and L. S. de B. Alves. On the existance of multiple self-excitation frequencies in the instability of interacting planar mixing layer and wake. In *31st Congress of the International Council of the Aeronautical Sciences*, Belo Horizonte, MG, Brazil, October 2018. ICAS. (Cited on pages 2, 9, and 11)

Y. Saad. *Iterative Methods for Sparse Linear Systems.* SIAM, 2nd edition, 2003. (Cited on page 6)

Ricado Dias dos Santos. *Um Estudo Sobre os Métodos de Runge-Kutta com Forte Estabilidade Linear e Não Linear.* PhD thesis, Universidade Federal Fluminense, 2020. (Cited on page 16)

H. Schlichting. *Boundary-Layer Theory.* MacGraw Hill, Inc., New York, 7th edition, 1986. (Cited on page 4)

P. J. Schmid and D. S. Henningson. *Stability and Transition in Shear-Flows.* Applied Mathematical Sciences. Springer & Verlag, New York, 2001. (Cited on page 5)

M. Schuabb, L. S. de B. Alves, and S. da C. Hirata. Two- and three-dimensional absolute instabilities in a porous medium with inclined temperature gradient and vertical throughflow. *Transport in Porous Media*, 132:135–155, 2020. (online). (Cited on page 5)

J. C. A. Silva. Grid shock alignment, boundary conditions axial symmetry and 3d simulations of hypersonic flows over blunt bodies. Master's thesis, Universidade Federal Fluminense, November 2023. (Cited on page 16)

D. Sipp and A. Lebedev. Global stability of base and mean flows: a general approach and its applications to cylinder and open cavity flows. *Journal of Fluid Mechanics*, 593:333–358, 2007. (Cited on page 4)

D. B. de Souza, R. B. Freitas, and L. S. de B. Alves. Criterion for the linear convective to absolute instability transition of a jet in crossflow: The countercurrent viscous and round mixing-layer analogy. *Physical Review Fluids*, 6(L041901), 2021. (Cited on page 5)

P. J. Strykowski and D. L. Niccum. The stability of countercurrent mixing layers in circular jets. *Journal of Fluid Mechanics*, 227:309–343, 1991. (Cited on page 1)

P. J. Strykowski and R. K. Wilcoxon. Mixing enhancement due to global oscillations in jets with annular counterflow. *AIAA Journal*, 31(3):564–570, 1993. (Cited on page 1)

A. Talamelli and I. Gavarini. Linear instability characteristics of incompressible coaxial jets. *Flow Turbulence and Combustion*, 76:221–240, 2006. (Cited on page 1)

R.de S. Teixeira and L. S.de B. Alves. Minimal gain marching schemes: Searching for unstable steady-states with unsteady solvers. *Theoretical and Computational Fluid Dynamics*, 31(5-6):607–621, 2017. (Cited on page 4)

V. Theofilis. Global linear instability. *Annual Review of Fluid Mechanics*, 43:319–352, 2011. (Cited on page 11)

B. Thiria and J. E. Wesfreid. Stability properties of forced wakes. *Journal of Fluid Mechanics*, 579:137–161, 2007. (Cited on page 4)

V. Tian, B. J. Mckeon, and I. A. Leyva. Split stream flow past a blunt trailing edge with application to combustion instabilities. In *48th AIAA/ASME/SAE/ASEE Joint Propulsion Conference & Exhibit*, number 2012-3807, Atlanta, GA, August 2012. AIAA. (Cited on pages 2 and 9)

E. Villermaux and H. Rehab. Mixing in coaxial jets. *Journal of Fluid Mechanics*, 425:161–185, 2000. (Cited on page 1)

D. Wallace and L. G. Redekopp. Linear instability characteristics of wake-shear layers. *Physics of Fluids A*, 4(1):189–191, 1992. (Cited on page 2)

S. Wolfram. *The Mathematica Book*. Wolfram Media. Cambridge University Press, New York, 5th edition, 2003. (Cited on pages 3, 4, and 5)